

rated crystals are present at depths as great as 675 m (9).

Intracellular calcification within the filaments of *P. dumetosus* is represented by elongate, doubly terminated aragonite crystals that average  $94 \pm 33 \mu\text{m}$  in length with an observed range of 48 to  $160 \mu\text{m}$  (Fig. 1C); these crystals range from 2 to  $6 \mu\text{m}$  in width. Identification of these crystals as aragonite has been confirmed by electron diffraction of single crystals and by x-ray diffraction of crystal aggregates. That these crystals are intracellular in origin is shown (i) in thin sections of capitular filaments where crystals are contained entirely within the cytoplasm (Fig. 1C) and (ii) by isolation of the cytoplasm and its included crystals through decalcification of the extracellular sheath. These large (48 to  $160 \mu\text{m}$ ) crystals of aragonite have been found only in *P. dumetosus* and may be of taxonomic value for the identification of this species. The presence of silt- to fine sand-sized, doubly terminated crystals of aragonite within lime sediments would possibly indicate a derivation from *P. dumetosus*.

RONALD D. PERKINS

Department of Geology,  
Duke University,  
Durham, North Carolina 27708

MICHAEL D. MCKENZIE\*

Department of Botany

PATRICIA LURIE BLACKWELDER  
Department of Zoology

#### References and Notes

1. R. K. Matthews, *J. Sediment. Petrology* **36**, 428 (1966).
2. T. W. Vaughn, *Geol. Soc. Amer. Bull.* **28**, 933 (1917); H. Gee, E. G. Moberg, D. M. Greenberg, R. Revelle, *Scripps Inst. Oceanogr. Bull. Tech. Ser.* **3**, 145 (1932); C. L. Smith, *J. Marine Res.* **3**, 147 (1940); P. E. Cloud and V. E. Barnes, *National Research Council Report, Treatise Marine Ecology and Paleontology No. 8* (1948), p. 29.
3. P. E. Cloud, *U.S. Geol. Surv. Prof. Pap. No. 350* (1962).
4. G. H. Drew, *Carnegie Inst. Wash. Publ. No. 182*, **5**, 7 (1914); C. B. Lipman, *ibid.* **No. 340**, **19**, 181 (1924); W. Bavendamm, *Ark. Mikrobiol.* **3**, 205 (1932); C. H. Openheimer, *Geochim. Cosmochim. Acta* **23**, 295 (1961); L. J. Greenfield, *Ann. N.Y. Acad. Sci.* **109**, 23 (1963).
5. H. A. Lowenstam, *J. Sediment. Petrology* **25**, 270 (1955).
6. N. D. Newell and J. K. Rigby, *Soc. Econ. Paleontol. Mineral. Spec. Publ.* **5**, 15 (1957).
7. K. W. Stockman, R. N. Ginsburg, E. A. Shinn, *J. Sediment. Petrology* **37**, 633 (1967).
8. D. S. Marszalek, *Proceedings of the Fourth Annual Scanning Electron Microscope Symposium*, Illinois Institute of Technology, Chicago (1971), p. 273.
9. S. C. Hastings, in preparation.
10. We thank K. M. Wilbur, R. B. Searles, and G. W. Lynts for helpful discussion and suggestions.

\* Present address: Department of Oceanography, Texas A & M University, College Station 77843.

2 August 1971; revised 18 October 1971

## Calcium Hydroxide: Its Role in the Fracture of Tricalcium Silicate Paste

**Abstract.** *The large areas of crystalline calcium hydroxide [Ca(OH)<sub>2</sub>] formed during the hydration of tricalcium silicate (Ca<sub>3</sub>SiO<sub>5</sub>) correspond to low-porosity regions in the hydrated paste. During the early stage of hydration, areas between Ca(OH)<sub>2</sub> crystals which consist of Ca<sub>3</sub>SiO<sub>5</sub> particles bonded together by calcium silicate hydrate represent the high-porosity portion of the paste. Because of the presence of Ca(OH)<sub>2</sub>, fracture in the hardened paste during this period propagates preferentially through the areas bonded by the calcium silicate hydrate phase and around the Ca(OH)<sub>2</sub> crystals. Calcium hydroxide also acts as a crack arrester. The influence of Ca(OH)<sub>2</sub> on fracture diminishes with increased hydration.*

Although portland cement concrete is the most widely used man-made building material in the world, microstructural factors which control fracture propagation through the hydrated cement paste are not completely understood. Of the four major constituents that make up portland cement, the most important is tricalcium silicate (Ca<sub>3</sub>SiO<sub>5</sub>) which is often used as a simplified model system to enable one to gain an understanding of the mechanisms controlling the hydration and engineering properties of portland cement. The Ca<sub>3</sub>SiO<sub>5</sub> reacts with water to form a poorly crystalline calcium silicate hydrate with high surface area and calcium hydroxide [Ca(OH)<sub>2</sub>]. Calcium silicate hydrate is considered to be more important in controlling the engineering properties of the hydrated system than Ca(OH)<sub>2</sub> which occurs predominantly as large crystals, often covering an area of over 0.1 mm<sup>2</sup> each.

The large size of the Ca(OH)<sub>2</sub> crystals renders them easily observable by standard techniques of optical microscopy. The preparation and in situ hydration of Ca<sub>3</sub>SiO<sub>5</sub> paste samples 40  $\mu\text{m}$  thick at a ratio of water to solids (by weight) (w/s) of 0.4, which is in the range of w/s ratios used for studies of engineering properties, made it possible to fracture samples at various degrees of hydration and to study by optical microscopy the role of Ca(OH)<sub>2</sub> in the propagation of fracture through the hydrated system.

The Ca<sub>3</sub>SiO<sub>5</sub> used in the study had a free lime content of < 0.1 percent (by weight) and a Blaine fineness of 4000 cm<sup>2</sup>/g (1). Samples were prepared by placing about 0.2 g of thoroughly mixed paste with a w/s ratio of 0.4 on a glass slide (7.6 by 2.5 by 0.16 cm). An identical slide was placed over the sample, and, by moving the two slides against one another, the paste was distributed evenly in a layer about 40  $\mu\text{m}$  thick. Excess paste was removed,

and the slides were sealed at the edges with paraffin. The samples were stored in an environment having a relative humidity of 100 percent at  $23^\circ \pm 2^\circ\text{C}$  until testing at 1, 3, 8, and 22 days.

Fracture was accomplished by three-point loading until failure occurred. Immediately after failure the sample, immersed in mineral oil to prevent drying, was studied by optical microscopy. Use of this technique ensured that the samples were fractured in a wet state and that the fracture pattern observed was due to mechanical stresses within the system rather than shrinkage.

The percentage of the total sample area covered by Ca(OH)<sub>2</sub> crystals at various degrees of hydration was determined by point counting. The reported Ca(OH)<sub>2</sub> areas include Ca<sub>3</sub>SiO<sub>5</sub> particles, calcium silicate hydrate, and gel pores entrapped within the Ca(OH)<sub>2</sub> crystals (2).

Tricalcium silicate reacts with water to form "inner-product" and "outer-product" calcium silicate hydrate and Ca(OH)<sub>2</sub> (3). The outer-product calcium silicate hydrate and crystalline Ca(OH)<sub>2</sub> form outside the original boundary of the Ca<sub>3</sub>SiO<sub>5</sub> grains, whereas the bulk of the calcium silicate hydrate occurs as inner product within the boundary of the original grain. Calcium hydroxide crystals grow around particles with which they come in contact. The particles entrapped within the Ca(OH)<sub>2</sub> crystals during the early stages of growth are only partially hydrated and may, indeed, never hydrate fully as they may be cut off from direct contact with the solution phase. At this stage the Ca(OH)<sub>2</sub> crystals are isolated from one another and represent low-porosity areas distributed throughout the groundmass. The space between the Ca(OH)<sub>2</sub> crystals is filled with Ca<sub>3</sub>SiO<sub>5</sub> particles which continue to hydrate. The Ca<sub>3</sub>SiO<sub>5</sub> particles are bound together by the outer-product calcium silicate hydrate which grows into the

space between particles and forms an interlocking mass. Relative to the  $\text{Ca}(\text{OH})_2$  areas, the porosity of the areas containing predominately  $\text{Ca}_3\text{SiO}_5$  particles is high during the early stages of hydration, as shown in Fig. 1, but decreases continuously with hydration. As hydration progresses, the  $\text{Ca}(\text{OH})_2$  crystals continue to grow and entrap more partially and completely hydrated  $\text{Ca}_3\text{SiO}_5$  particles and calcium silicate hydrate. The space between particles into which the  $\text{Ca}(\text{OH})_2$  can grow decreases as the time of hydration increases, since this space is being filled with the outer-product calcium silicate hydrate. Therefore, as one goes out from the original nucleus of a  $\text{Ca}(\text{OH})_2$  crystal, the amount of entrapped matter increases at a greater than linear rate; however, even when there is a large amount of entrapped matter, the  $\text{Ca}(\text{OH})_2$  at the edges of the crystal maintains crystal orientation as determined by its optical continuity with the bulk of the crystal. As growth of the  $\text{Ca}(\text{OH})_2$  continues, the crystals begin to interfere with each other's growth, and, at late stages of hydration in systems with low w/s ratios, the crystal areas come in contact with one another.

The hydration of the  $\text{Ca}_3\text{SiO}_5$  paste proceeded normally on the slides along with the nucleation and growth of  $\text{Ca}(\text{OH})_2$  crystals throughout the bulk of the paste. The crystals initially grow in all directions until reaching the thickness of the section after which growth continues laterally at the constant section thickness. Cracks were not present in the samples prior to testing. After testing, microcracks radiating from the

primary fracture were studied. The number of microcracks observable after stress was released diminished with increased hydration. At 8 days, only two microcracks large enough for study were present. Therefore, samples hydrated longer than 8 days were also point-loaded under compression to provide a greater number of microcracks.

The position of fractures in the paste was undoubtedly influenced by the fracture of the glass slide or boundary layer. However, fracture patterns in the paste at 1 and 3 days were the same, no matter whether plastic or glass slides were used, even though plastic slides were not fractured during loading. Plastic slides were not used throughout the study because of difficulties encountered in sealing the slides with paraffin to prevent drying of the paste. The similarity in the paste fracture pattern with different slide materials indicates that the paste microstructure rather than the boundary layer materials influenced the fracture within the paste.

Fractures in the  $\text{Ca}_3\text{SiO}_5$  paste samples hydrated for 1, 3, 8, and 22 days are shown in Fig. 2. After hydration for 1 day  $\text{Ca}(\text{OH})_2$  covers about 29 percent (by volume) of the paste area (2). The fracture path goes around the  $\text{Ca}(\text{OH})_2$  crystals and preferentially through the outer-product calcium silicate hydrate which bonds the  $\text{Ca}_3\text{SiO}_5$  particles together (Fig. 2A). The fracture deviates around the  $\text{Ca}(\text{OH})_2$  crystals in a tortuous path instead of passing through them. The mechanical strength of the system at this stage of hydration must be deter-

mined by the interlocked calcium silicate hydrate foils which are holding the  $\text{Ca}_3\text{SiO}_5$  particles together. However, the tortuous fracture path caused by the presence of  $\text{Ca}(\text{OH})_2$  means that additional energy must be supplied to the system to cause failure. After 3 days, the  $\text{Ca}(\text{OH})_2$  crystal areas cover 42 percent of the paste area. The fracture path still passes preferentially around  $\text{Ca}(\text{OH})_2$  crystals (Fig. 2B). In some cases (Fig. 2, E and F), the fracture terminates at  $\text{Ca}(\text{OH})_2$  crystals or intersects a  $\text{Ca}(\text{OH})_2$  crystal and creates several new branch fractures before propagating further through the paste. In these cases the  $\text{Ca}(\text{OH})_2$  is acting as a crack arrester (Fig. 2E) which toughens the hydrated system since it takes additional energy to generate new crack formation.

After 8 days, the  $\text{Ca}(\text{OH})_2$  crystals cover about 60 percent of the paste area. The space between crystals is diminished, and in many areas crystals have come in contact with one another. The fracture path, shown in Fig. 2C, still preferentially goes through the area bound together by the calcium silicate hydrate. A larger number of the  $\text{Ca}(\text{OH})_2$  crystals are fractured; however, the fracture tends to go through the extremities rather than the core of the  $\text{Ca}(\text{OH})_2$  crystals. These areas contain a greater amount of entrapped material than the core of the crystals.

After 22 days,  $\text{Ca}(\text{OH})_2$  crystals cover about 80 percent of the paste area. Fracture, when it occurs, must pass through many of the crystal areas as it is virtually impossible to define a

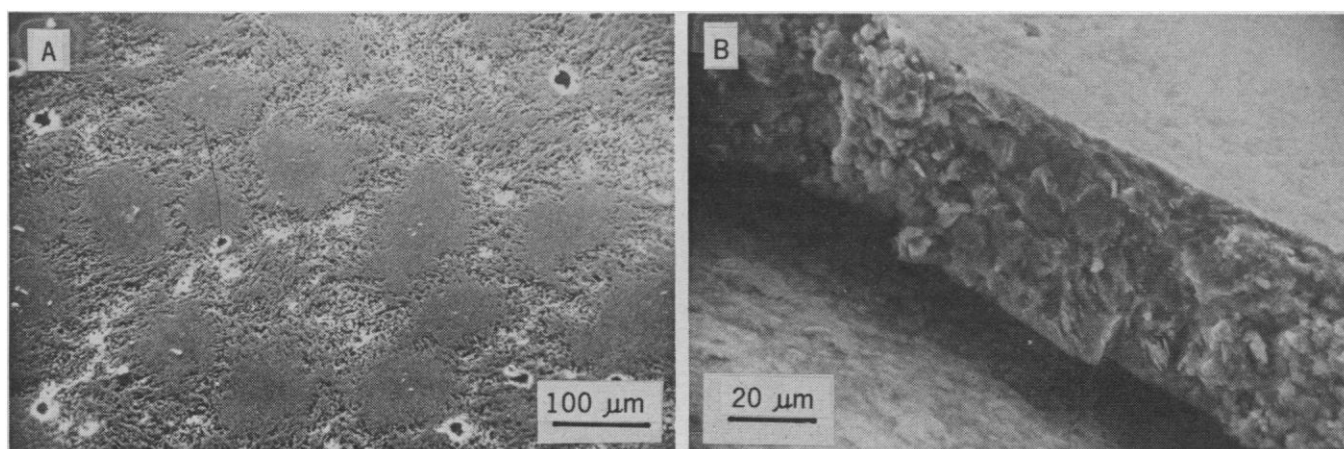


Fig. 1. (A) Scanning electron micrograph of a thin section surface of  $\text{Ca}_3\text{SiO}_5$  paste hydrated for 3 days. The dense areas are composed of  $\text{Ca}(\text{OH})_2$ , whereas the porous areas consist of  $\text{Ca}_3\text{SiO}_5$  particles and calcium silicate hydrate. The compositional identity of the two areas was confirmed by means of elemental analysis with a nondispersive x-ray analyzer attachment on the scanning electron microscope. (B) Cross section of a thin section showing a low-porosity  $\text{Ca}(\text{OH})_2$  area in the center with adjacent areas of higher porosity containing  $\text{Ca}_3\text{SiO}_5$  and calcium silicate hydrate.

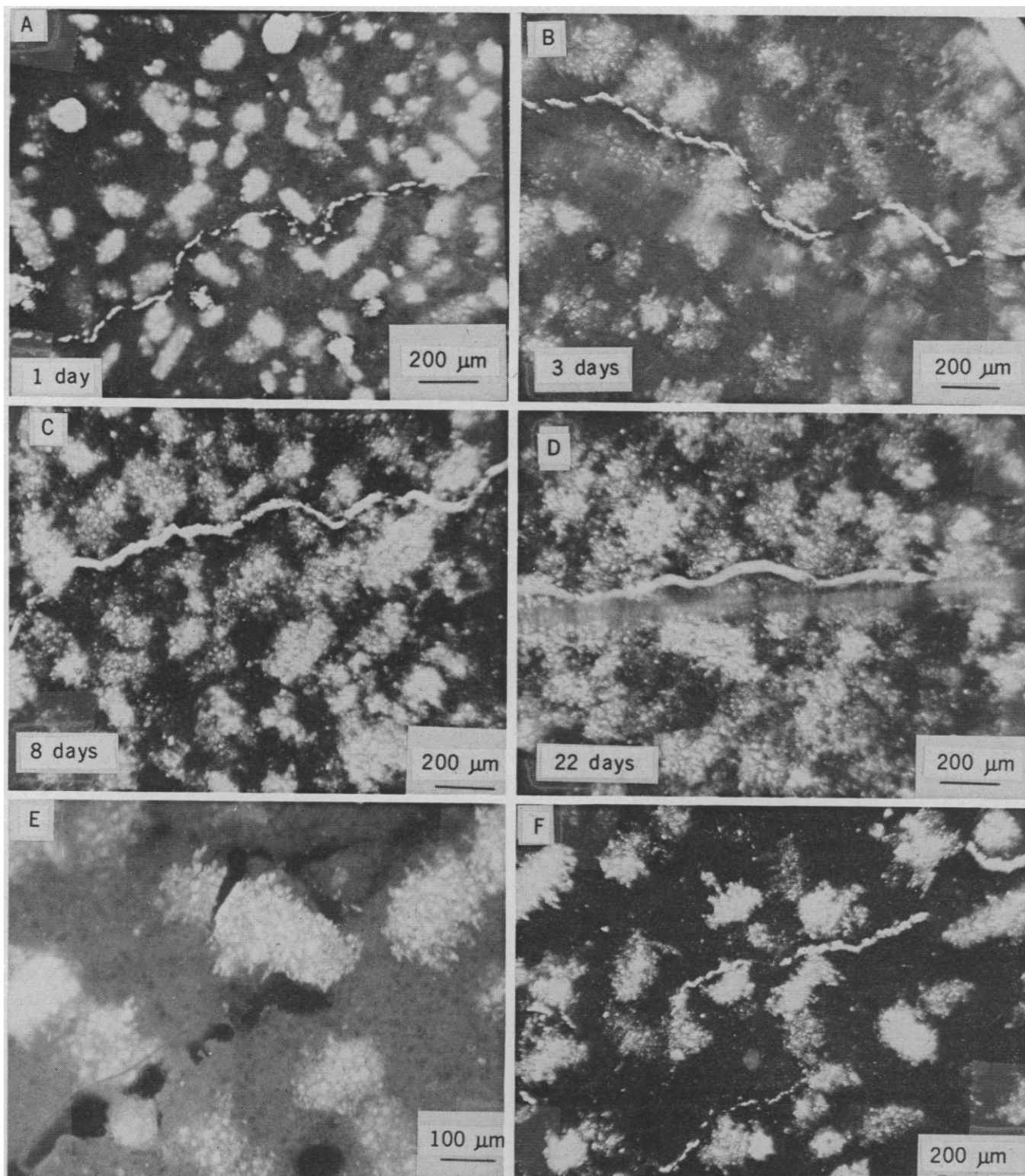


Fig. 2. Tricalcium silicate pastes with a w/s ratio of 0.4 hydrated at 23°C for 1, 3, 8, 22, and 3 days, as shown in (A), (B), (C), (D), and (E), respectively. Except where noted, the microscope polarizers were set at approximately 80° to one another, and the fractures appear as white irregular lines. The light areas are  $\text{Ca(OH)}_2$  crystals, and the bright spots within the crystals are entrapped  $\text{Ca}_2\text{SiO}_5$  particles. The dark groundmass contains  $\text{Ca}_2\text{SiO}_5$  particles, calcium silicate hydrate, and water in the space between particles. The hazy straight lines approximately parallel to the fracture in (B) and (D) are due to cracks in the glass slides which occurred during testing. The fracture initially goes around the  $\text{Ca(OH)}_2$  areas, as shown in (A) and (B), but with increased time of hydration the fracture path, as shown in (C) and (D), passes through an increasing number of  $\text{Ca(OH)}_2$  crystals. Crystals of  $\text{Ca(OH)}_2$  also act as crack arresters in the paste, as shown in (E). The fracture appears as a dark area transverse the photo, and it propagated from upper right to lower left. The fracture encountered a  $\text{Ca(OH)}_2$  crystal which necessitated the formation of new branch fractures and the splitting of  $\text{Ca(OH)}_2$  along a basal crystallographic plane. As seen in (F), fractures still go around  $\text{Ca(OH)}_2$  crystals in a  $\text{Ca}_2\text{SiO}_5$  paste with a w/s ratio of 0.7 hydrated for 20 days. The lower fracture is arrested by a  $\text{Ca(OH)}_2$  crystal.

path through an area not containing  $\text{Ca}(\text{OH})_2$  (Fig. 2D).

Further hydration results in the extension of  $\text{Ca}(\text{OH})_2$  areas as well as a strengthening and densification of the calcium silicate hydrate zones. This densification reduces the difference in strength between the two hydrated phases and makes the properties of the paste more uniform on a microstructural scale. Fracture within the system propagates along a more direct path as differences in the microstructural components decrease.

An increase in the w/s ratio increases the porosity of the  $\text{Ca}_3\text{SiO}_5$  particle areas but does not change the porosity of the  $\text{Ca}(\text{OH})_2$  crystals. However, the distance between  $\text{Ca}(\text{OH})_2$  crystals increases and the degree to which the crystals grow together decreases as the w/s ratio increases. As a result of these factors, the fracture continues to go through the calcium silicate hydrate zones and around  $\text{Ca}(\text{OH})_2$  at later ages (increased degrees of hydration). For example, in a sample with a w/s ratio of 0.7 hydrated for 20 days, the  $\text{Ca}(\text{OH})_2$  covers about 35 percent of the paste area and the fracture still goes around the  $\text{Ca}(\text{OH})_2$  crystals (Fig. 2F).

The relevance of the fracture observed in the paste sections to that of bulk samples may be questioned. However, the fracture surface of the thin sections of the paste at early stages of hydration would contain a preponderance of calcium silicate hydrate, in agreement with observations by scanning electron microscopy made by Young and Lawrence (4) of the fracture surface of bulk  $\text{Ca}_3\text{SiO}_5$  paste samples.

A completely hydrated  $\text{Ca}_3\text{SiO}_5$  paste contains about 42 percent  $\text{Ca}(\text{OH})_2$ , as compared to 25 percent in ordinary portland cement paste. In addition, the  $\text{Ca}(\text{OH})_2$  crystals in portland cement paste are smaller and have more of a platy habit because of the presence of sulfate and other ions in solution. Although the quantity and morphology of  $\text{Ca}(\text{OH})_2$  differ in the two systems, the influence of  $\text{Ca}(\text{OH})_2$  on fracture propagation would be expected to be the same since it represents low-porosity areas in both systems.

RICHARD L. BERGER

Department of Civil Engineering,  
University of Illinois,  
Urbana 61801

#### References and Notes

1. *Book Amer. Soc. Test. Mater. Stand.* 9, 207 (1968), standard C204-68.
2. The apparently large areal coverage of  $\text{Ca}(\text{OH})_2$  includes engulfed  $\text{Ca}_3\text{SiO}_5$  particles, calcium silicate hydrate, and gel pores. If we use a density of 2.2 g/cm<sup>3</sup> for both  $\text{Ca}(\text{OH})_2$  and calcium silicate hydrate, the total volume of hydrated solid would be approximately 56 cm<sup>3</sup> starting with 100 g of  $\text{Ca}_3\text{SiO}_5$ . This corresponds to about 79 percent of the total volume of the original mix with a w/s ratio of 0.4 (40 ml of H<sub>2</sub>O and 31 cm<sup>3</sup> of  $\text{Ca}_3\text{SiO}_5$ ). Since the  $\text{Ca}(\text{OH})_2$  grows in the space between particles, it can at late stages of hydration appear to cover much of the sample area. In addition, the excess paste squeezed from the slide during preparation appeared to have a higher w/s ratio than that left on the slide. The lower porosity paste system on the slide would result in less space to be filled by the  $\text{Ca}(\text{OH})_2$ , and thus a higher areal coverage by the  $\text{Ca}(\text{OH})_2$ .
3. J. H. Taplin, *Aust. J. Appl. Sci.* 10, 329 (1959).
4. J. F. Young and F. V. Lawrence, paper presented at the 73rd annual meeting of the American Ceramic Society, Chicago, Illinois, 1971.

1 June 1971; revised 18 November 1971

## Uranium in Runoff from the Gulf of Mexico Distributive Province: Anomalous Concentrations

**Abstract.** *Uranium concentrations in North American rivers are higher than those reported 20 years ago. The increase is attributed to applications to agricultural land of larger amounts of phosphate fertilizer containing appreciable concentrations of uranium. Experiments showing a constant phosphorous-uranium ratio for various types of fertilizers and for the easily solubilized fraction of 0-46-0 fertilizers support this view.*

High uranium concentrations are reported for present-day North American rivers relative to those found 10 to 20 years ago for the same rivers or for rivers in other parts of the world draining less intensively cultivated areas. This anomaly has been attributed to high concentrations of uranium thought to be present in phosphate fertilizers (1, 2). Lack of knowledge of uranium depletion or enrichment in the various stages of fertilizer production and of the behavior of uranium during weathering of a fertilized soil has made these observations rather speculative. This report describes experiments designed to

answer these questions and attempts to evaluate the pollution potential of uranium, a heavy metal whose toxic levels in organisms are similar to those of mercury and lead.

Uranium concentrations were determined by a delayed neutron technique (3). The method is nondestructive, rapid (about 5 minutes), and precise (sigma is about 5 percent for a single determination on a 2-g solid sample with about 1 ppm). Briefly, samples are weighed into a polyethylene vial which is inserted into a "rabbit." The "rabbit" is blown into a flux of neutrons (about 10<sup>12</sup> neutrons cm<sup>-2</sup> sec<sup>-1</sup> in this case) via a pneumatic system for 1 minute, removed, allowed to cool for 30 seconds, and then counted for 1 minute with BF<sub>3</sub> neutron counters in a 4π arrangement. Sample activities are compared with standards treated in the same manner.

River and other aqueous samples were filtered through 0.8-μm Millipore filters and evaporated to dryness. The dried solids were treated as described above. Concentrations were determined on the basis of the sample volume and total weight of dissolved solids.

Uranium concentrations for 22 samples taken from 15 different rivers that flow into the Gulf of Mexico are shown in Fig. 1. Most samples have considerably higher concentrations than were found years ago in several North American rivers (4). High uranium in the Rio Grande, Nueces, Frio-Atascosa,

Table 1. Spring 1971 distribution of uranium versus phosphate in the Brazos River and its tributaries.

| Collection date (1971)     | Phosphate (μg/l liter) | Uranium (μg/l liter) | P/U ratio |
|----------------------------|------------------------|----------------------|-----------|
| <i>Brazos River</i>        |                        |                      |           |
| 3-12*                      | 36.10                  | 1.16                 | 31.0      |
| 3-25†                      | 130.0                  | 1.48                 | 88.0      |
| 4-16‡                      | 46.0                   | 1.51                 | 30.4      |
| 4-17§                      | 62.0                   | 1.32                 | 47.0      |
| 4-21*                      | 10.8                   | 1.88                 | 10.8      |
| 5-4                        | 41.9                   | 1.90                 | 22.0      |
| 5-6*                       | 64.3                   | 2.07                 | 31.6      |
| 5-11‡                      | 53.5                   | 0.94                 | 57.0      |
| 5-25§                      | 28.0                   | 2.70                 | 10.4      |
| <i>Little Brazos River</i> |                        |                      |           |
| 3-12*                      | 60.5                   | 0.69                 | 87.5      |
| 3-25†                      | 48.8                   | 1.27                 | 38.2      |
| <i>Navasota River</i>      |                        |                      |           |
| 5-11‡                      | 234.5                  | 2.01                 | 116.0     |

\* After storm. † No rain. ‡ Rain, about 1 inch. § Showers. || Dry for 2 weeks.